



Vortex dynamics controlled by pinning centers on Nb superconductor open microtubes



R.O. Rezaev^{a,b}, V.M. Fomin^{c,*}, O.G. Schmidt^{c,d}

^a Moscow Engineering Physics Institute, Kashirskoe Shosse 31, Moscow 115409, Russia

^b Tomsk Polytechnic University, Lenin Ave. 2, Tomsk 634050, Russia

^c Institute for Integrative Nanosciences, IFW Dresden, Helmholtzstraße 20, 01069 Dresden, Germany

^d University of Technology Chemnitz, Reichenhainer Straße 70, 09126 Chemnitz, Germany

ARTICLE INFO

Article history:

Received 11 August 2013

Received in revised form 8 October 2013

Accepted 9 October 2013

Available online 16 October 2013

Keywords:

Flux pinning

Nanostructured materials

Niobium

Type II superconductors

ABSTRACT

Vortex dynamics on a Nb superconductor open microtube are studied theoretically taking into account the impact of single and multiple pinning centers. These dynamics are described by two characteristic times: the period of nucleation of vortices at one edge of the tube and the duration of motion of a vortex along the tube. Simulation reveals that the both characteristic times change by a factor of up to two due to the presence of pinning centers. Different regimes of vortex dynamics are effectively controlled by varying positions of pinning centers at given values of the applied magnetic field, the tube radius and the transport current orthogonal to the tube axis. An experimental detection of the tube curvature effects on vortex dynamics stays feasible in the presence of pinning centers.

© 2013 Elsevier B.V. All rights reserved.

1. Introduction

Phenomena connected with the behavior of Abrikosov vortices in the presence of different kinds of defects (natural or artificial) such as a ratchet effect, a matching field effect, change of the spectrum of core excitations of a vortex, Majorana states in the pinned vortices have been extensively studied (see, for instance, Refs. [1–4]). It is shown, for example, that the controlled insertion of artificial pinning sites in type-II superconductors allows for manipulating the motion of superconducting vortices in the presence of a transport current [5,6]. Introduction of artificial micro- or nano-holes (antidots) in superconducting films is based on the methods of optical lithography and ion-beam etching [6–11]. Random, periodic (triangular) or quasiperiodic (Penrose) arrays of antidots lead to diverse vortex patterns in superconducting Nb films [12]. Stationary distribution of vortices as well as vortex dynamics have been studied using different experimental techniques, such as the magneto-optical scanning holographic electron microscopy [13], the Hall sensor method [11] and the laser scanning microscopy [14]. Superconducting properties substantially depend on the dimensionality of a sample [15]. Achievements in fabrication [16–19] of rolled-up materials make it possible to fabricate cylindrical tubes of superconducting materials (e.g., Nb) of radius about

500 nm from a planar film of thickness about 50 nm. With the roll-up technique, the quasi-2-dimensionality of the film is combined with a curvature. As shown in Ref. [16], the vortex dynamics are significantly determined by the curvature of the superconductor at the nano- or microscale. The present work is aimed at a quantitative analysis of the simultaneous effects of curvature and pinning centers on vortex dynamics on an open superconductor microtube.

2. Model

We consider a Nb superconductor open tube [16] of radius R and length L (Fig. 1a). There are two paraxial contacts on the edges of the tube slit, which are presented in Fig. 1a by heavy red lines along the tube. A transport current is applied through the contacts and flows orthogonal to the axis along the surface (circular red lines). Such contacts cause vortex dynamics in the paraxial direction unlike those in the direction orthogonal to the tube axis considered in Ref. [20]. The system is in a magnetic field perpendicular to the axis. Our model is based on the time-dependent Ginzburg–Landau (GL) equation [21] for the order parameter ψ in the dimensionless form [22]

$$\frac{\partial \psi}{\partial t} = (\nabla - i\mathbf{A})^2 \psi + 2\kappa^2 \psi (1 - |\psi|^2), \quad (1)$$

where κ is the GL parameter, ∇ is the gradient operator. The normal to the cylindrical surface component of the magnetic field, according to Fig. 1a, is $B_n = -B \sin(\varphi)$. The effective magnetic flux is

* Corresponding author. Tel.: +49 351 4659 780.

E-mail addresses: rezaev.roman@cadegis.com (R.O. Rezaev), v.fomin@ifw-dresden.de (V.M. Fomin), o.schmidt@ifw-dresden.de (O.G. Schmidt).

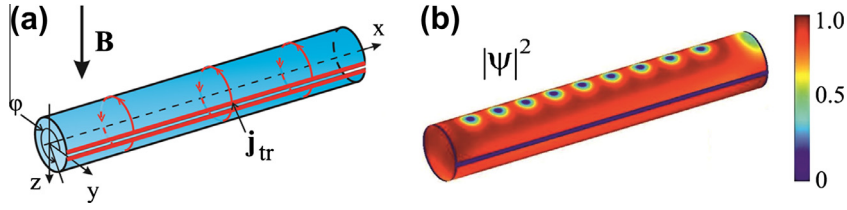


Fig. 1. (a) Schematic view of an open tube. The electrodes are displayed by the heavy red lines. The x -axis is the longitudinal axis of the cylindrical coordinate system (ρ, ϕ, x) . The angle ϕ is counted from the positive direction of the y -axis, passing through the middle of the slit. $\mathbf{B} = B\mathbf{e}_x$ is the external magnetic field. (b) Distribution of the squared amplitude of the order parameter $|\psi|^2$. Vortices nucleate at the top half-cylinder at the right edge, move in the direction opposite to the x -axis and denudeate at the left edge. The opposite dynamics occurs at the bottom half-cylinder [16]. (For interpretation of the references to color in this figure legend, the reader is referred to the web version of this article.)

$\Phi = 2RLB$ and the vector potential is taken in the Landau gauge: $\mathbf{A} = A\mathbf{e}_x$, $A = -By$. We neglect the magnetic field induced by superconducting currents because according to our calculations it is one order of magnitude lower than the applied magnetic field. Since our evaluation shows that in the tube under analysis the scalar potential concentrates mainly in the region far away from the region with moving vortices, its influence on the vortex dynamics can be disregarded in the first approximation. Boundary conditions for Eq. (1) are [16]:

$$\begin{aligned} (\nabla - i\mathbf{A})\psi|_{n,\text{boundary}} &= 0, \\ \left[\nabla - i(\mathbf{A} + \mathbf{j}/|\psi|^2) \right] \psi|_{n,\text{electrode}} &= 0, \end{aligned} \quad (2)$$

where \mathbf{j} is the transport current density, i is the imaginary unit. Input data for the subsequent calculations are presented in Table 1 (data are taken from Refs. [16,22]) and Table 2 (Φ_0 is the magnetic flux quantum). In the external magnetic field and without a transport current, a stationary distribution of the order parameter occurs in the tube. The vortices are located on the opposite sides of the tube [16]. When the transport current is switched on, the vortices start to move under the Magnus force. A quasistationary regime is established at some values of the transport current density and the magnetic field. In this regime vortices nucleate periodically at one of the edges of the tube, move in the paraxial direction and then denudeate at the other edge of the tube. According to Fig. 1b,

vortices move to the left (to the right) on the top (bottom) side of the tube with respect to the x -direction. A snapshot of the distribution of the order parameter is presented on Fig. 1b (see Ref. [16]). Physical validation of the model and evaluation of the “longitudinal” (parallel to the applied transport current direction) electric field through the Hall voltage generated between the points in the xy -plane on both sides on the slit as a detectable measure of the vortex dynamics are provided in Ref. [16].

For our simulation of vortex dynamics, different characteristics of pinning centers are reduced to size and strength (the measure of the force acting on the vortex). It is known [23] that a pinning center influences the vortex dynamics most effectively when its size is about the coherence length ξ . If the pinning center is smaller than ξ , the superconducting order parameter does not vary substantially in the region of the pinning center [23]. Due to the 3D–2D pinning crossover (a transition from the 3D thickness-independent pinning to the 2D pinning), we suggest that for our structure the most important pinning factors are the surface roughness and impurities. Temperature fluctuations do not influence the vortex state strongly in low- T_c superconductors [24]. For the numerical study of the 2D pinning, the collective pinning theory [25] was developed using the molecular dynamics methods (see, for example, [26]). In the framework of the GL approach, modeling of a pinning center through a spatial variation of the GL parameter is advantageous as it represents the attracting (repelling) action of pinning centers on vortex motion. Following this idea, we model an attracting pinning center by assuming the Gaussian spatial inhomogeneity of the GL parameter:

$$\kappa(\mathbf{r}) = \kappa_{\text{Nb}} \left\{ 1 - N \exp \left[-(\mathbf{r} - \mathbf{r}_0)^2 / 2\sigma^2 \right] \right\}, \quad (3)$$

where κ_{Nb} is the GL parameter of the Nb matrix in the dirty limit [16]; \mathbf{r}_0 is the position of the pinning center on the tube; σ is a parameter characterizing the size of the pinning center; in our calculation we take $\sigma = \xi$. The phenomenological parameter $N \in [0, 1]$ defines the strength of the pinning center. For the selected parameters, a conspicuous effect of one pinning center is observed when $N = 1$. We have numerically checked that all effects of the pinning centers on the vortex dynamics described below are protected by the geometry of the open tube and are qualitatively robust with respect to different models of pinning centers. In order to optimize the modeling of pinning centers, sample-specific experimental data are needed.

3. Interaction of a vortex with a pinning center on a tube

To quantify the influence of pinning centers on the vortex dynamics, we introduce, following Ref. [16], two characteristic times: the duration of motion of the vortex along the tube Δt_1 and the time interval between two successive nucleations of vortices at one edge Δt_2 . The latter is the period of nucleation of vortices at one edge of the tube. Without pinning centers, the characteristic

Table 1
Physical and geometrical parameters used for simulation.

	Notation	Value
Penetration depth	λ	279 nm
Coherence length	ξ	56 nm
GL parameter	$\kappa = \lambda/\xi$	5
Fermi velocity	v_F	6×10^5 m/s
Thickness of the film (used only for the free electron path calculation)	d	50 nm
Free electron path [30]	$l = 10/(1 + 40 \text{ (nm)}/d)$	5.6 nm
Diffusion coefficient	$D = lv_F/3$	11.2×10^{-4} m ² s ⁻¹
Relative temperature	T/T_c	0.95

Table 2
Definition of dimensionless units used for Eqs. (1) and (2).

	Unit	Value
Time	$2\lambda^2/D$	0.14 ns
Length	$\sqrt{2}\lambda$	395 nm
Magnetic field	$\Phi_0/(4\pi\lambda)$	2.12 mT
Magnetic flux	Φ_0	
Current density	$\Phi_0/(8\sqrt{2}\pi^2\lambda^3)$	8.57×10^9 A m ⁻²

Download English Version:

<https://daneshyari.com/en/article/8164624>

Download Persian Version:

<https://daneshyari.com/article/8164624>

[Daneshyari.com](https://daneshyari.com)